

# Mast cells and dendritic cells form synapses that facilitate antigen transfer for T cell activation

Amanda Carroll-Portillo,<sup>1</sup> Judy L. Cannon,<sup>1,2,3</sup> Joost te Riet,<sup>4</sup> Anna Holmes,<sup>1</sup> Yuko Kawakami,<sup>5</sup> Toshiaki Kawakami,<sup>5,6</sup> Alessandra Cambi,<sup>4</sup> and Diane S. Lidke<sup>1,3</sup>

<sup>1</sup>Department of Pathology and <sup>2</sup>Department of Molecular Genetics and Microbiology, The University of New Mexico School of Medicine, Albuquerque, NM 87131

<sup>3</sup>Cancer Research and Treatment Center, The University of New Mexico, Albuquerque, NM 87131

<sup>4</sup>Department of Tumor Immunology, Radboud Institute for Molecular Life Sciences, Radboud University Medical Center, 6525 GA Nijmegen, Netherlands

<sup>5</sup>Division of Cell Biology, La Jolla Institute for Allergy and Immunology, La Jolla, CA 92037

<sup>6</sup>Laboratory for Allergic Disease, RIKEN Center for Integrative Medical Sciences (IMS-RCI), Tsurumi-ku, Yokohama 230-0045, Japan

Mast cells (MCs) produce soluble mediators such as histamine and prostaglandins that are known to influence dendritic cell (DC) function by stimulating maturation and antigen processing. Whether direct cell–cell interactions are important in modulating MC/DC function is unclear. In this paper, we show that direct contact between MCs and DCs occurs and plays an important role in modulating the immune response. Activation of MCs through Fc $\epsilon$ RI cross-linking triggers the formation of stable cell–cell interactions with immature DCs that are reminiscent of the immunological synapse. Direct cellular contact differentially regulates the secreted cytokine profile, indicating that MC modulation of DC populations is influenced by the nature of their interaction. Synapse formation requires integrin engagement and facilitates the transfer of internalized MC-specific antigen from MCs to DCs. The transferred material is ultimately processed and presented by DCs and can activate T cells. The physiological outcomes of the MC–DC synapse suggest a new role for intercellular crosstalk in defining the immune response.

## Introduction

Immune system function requires a complex network of intercellular communication between distinct cell types, involving both soluble mediators and direct cell–cell contacts. For example, upon activation, mast cells (MCs) secrete a variety of cytokines, chemokines, prostaglandins, and other inflammatory mediators that are known to regulate the function of other immune cells (Caron et al., 2001b; Skokos et al., 2003; Suto et al., 2006; Dawicki et al., 2010). Furthermore, physical interactions between dendritic cells (DCs) and immune cells other than classical T lymphocytes (i.e., neutrophils/DCs, NK [natural killer] cells/DCs, and NK-T cells/DCs) are being discovered, thus broadening the repertoire of DC-interacting partners contributing to the establishment of an immune response (Yang et al., 2000; van Gisbergen et al., 2005c; Valentin-Torres et al., 2012).

Recognized as sentinels of the immune system, DCs and MCs (Lozewicz et al., 1990; Leslie, 2007) localize to similar peripheral tissues (skin and mucosae) and serve immunoregulatory and effector functions, respectively. MCs express the high affinity IgE receptor, Fc $\epsilon$ RI, and are best known for their role in allergy and asthma. However, MCs also express receptors capa-

ble of recognizing pathogens (such as Toll-like receptors) and have been implicated in many physiological responses, including rheumatoid arthritis, arteriosclerosis, and cancer (Leslie, 2007). Recently, members of our group have demonstrated that MCs form a synapse in response to an antigen-presenting bilayer (Carroll-Portillo et al., 2010; Spendier et al., 2010) and can interact with DCs (Carroll-Portillo et al., 2012). It is becoming clear that MCs play a more complex role in the overall immune response than previously recognized. Immature DCs (imDCs) reside in the tissue, capturing and processing antigen for development of tolerance or disease response. There are several DC subsets (myeloid DCs, Langerhans cells, plasmacytoid DCs, dermal DCs, etc.) with phenotypic differences, increasing the functional complexity of these cells (Shortman and Liu, 2002). Upon stimulation with non-self-antigen or inflammatory cytokines, DCs begin maturation and traffic to the draining lymph node. Within the lymph node, DCs present captured antigen to T cell populations, stimulating proliferation and subsequent immune responses (Morva et al., 2012; Dalod et al., 2014).

As MCs and DCs reside in close proximity at environmental interfaces, their capacity for crosstalk has been documented (Allam et al., 2008; Dawicki et al., 2010; Dudeck et al., 2011).

Correspondence to Diane S. Lidke: [dlidke@salud.unm.edu](mailto:dlidke@salud.unm.edu)

Abbreviations used in this paper: actMC, activated MC; AF, Alexa Fluor; AFM, atomic force microscopy; BMDC, bone marrow-derived DC; BMMC, bone marrow-derived MC; DC, dendritic cell; F–D, force–distance; GPI, glycosyl-phosphatidylinositol; IHC, immunohistochemistry; imDC, immature DC; LPS, lipopolysaccharide; MC, mast cell; MTOC, microtubule-organizing center; OVA, ovalbumin; PMC, peritoneal-derived MC.

© 2015 Carroll-Portillo et al. This article is distributed under the terms of an Attribution-Noncommercial-Share Alike-No Mirror Sites license for the first six months after the publication date (see <http://www.rupress.org/terms>). After six months it is available under a Creative Commons License (Attribution-Noncommercial-Share Alike 3.0 Unported license, as described at <http://creativecommons.org/licenses/by-nc-sa/3.0/>).

In particular, MC-derived soluble factors have been shown to affect DC functions such as activation, migration to lymph nodes, and Th2 polarization (Caron et al., 2001a; Mazzoni et al., 2006; Suto et al., 2006; Shelburne et al., 2009; Dawicki et al., 2010; Reuter et al., 2010; de Vries et al., 2011). Communication between MCs and DCs has also been shown to regulate other lymphocytes including T cells and B cells (Skokos et al., 2003; Mazzoni et al., 2006; de Vries et al., 2011; Dudeck et al., 2011). Supernatants from activated MCs initiate both mouse and human DC maturation, increase CCL21 chemotaxis to the draining lymph nodes, and result in generation of Th2-promoting DCs as well as a Th2 centric immune response (Caron et al., 2001a; Kitawaki et al., 2006; Mazzoni et al., 2006). MC cytokines, such as TNF and granulocyte macrophage colony-stimulating factor, recruit DCs to sites of infection and increase the longevity of imDCs contributing to allograft tolerance (Suto et al., 2006; Shelburne et al., 2009; Reuter et al., 2010; de Vries et al., 2011). Although a physical MC–DC interaction has been predicted (Kitawaki et al., 2006; Dudeck et al., 2011), formal demonstration of direct cellular contact between MCs and DCs has been lacking. Furthermore, the mechanisms that underlie MC–DC contact and the physiological outcomes of such interactions remain poorly defined.

In this study, we have combined live-cell imaging techniques with immunological and biochemical assays to unravel the mechanisms and dynamics of MC–DC interplay. We show that MCs and DCs form synapses that are dependent on MC activation and integrin engagement. These direct interactions stimulate changes in the secretion profile of select cytokines. We also find that MC–DC synapse formation facilitates transfer of endosomal contents, including antigen and membrane, from activated MCs (actMCs) to imDCs. Furthermore, DCs are capable of processing and presenting the transferred antigen that ultimately results in the activation of T cells. Together, these results demonstrate that there is a complex interplay between soluble cues and intercellular crosstalk that fine-tunes the immune response.

## Results

### Direct contact of MCs and DCs is observed in tissue

MCs and DCs are known to localize to the same tissues. We used immunohistochemistry (IHC) to assess whether MCs and DCs are found within close proximity in human tissue. 5- $\mu$ m sections of normal human colon, intestine, lung, skin, and tonsil were each obtained from five different donors and labeled to detect MCs (Fig. 1 A, tryptase, brown; Walls et al., 1990) and DCs (Fig. 1 A, DC-SIGN, pink; Bergman et al., 2004; van Gisbergen et al., 2005a,c). Labeling of tonsil tissue served as the control, and negative controls were run with all IHC reactions (Fig. S1). IHC revealed that it is common to find MCs and DCs in close proximity (Fig. 1 A, arrows). To quantify the potential for cell–cell contacts, we determined the percentage of MCs that were immediately adjacent to a DC and found this value to be consistently high across all donors and tissue types (Fig. 1 B). It should be noted that in addition to DCs, there are other cells that express DC-SIGN, such as alveolar macrophages (Soilleux et al., 2002). However, within the multiple subsets of DCs, DC-SIGN<sup>+</sup> DCs have been detected in the dermal layer of the skin (Geijtenbeek et al., 2000), intestine

(Jameson et al., 2002), colon (Soilleux et al., 2002), and lung (de Witte et al., 2008), thus motivating the use of this marker in the IHC experiments. These results confirm that MCs and DCs are found within close proximity and suggest that direct MC–DC interactions could occur *in vivo*.

### MC–DC interactions alter cytokine production

As immune modulators, both MCs and DCs are capable of secreting a wide variety of cytokines to stimulate or repress immune responses. To determine whether direct cell–cell interactions might influence cellular responses, cytokine secretion was measured using ELISA. MCs and imDCs were co-incubated to allow for either direct or indirect (with transwell separation) interactions. To activate MCs, Fc $\epsilon$ RI signaling was initiated by the addition of the multivalent antigen, DNP-BSA, which cross-links the DNP-specific IgE bound to the receptor. Supernatants from 2- and 12-h co-cultures were collected for ELISAs. Of the cytokines tested (IL1ra, MIP1 $\alpha$ , MCP-1, IL-4, IL-6, IL-10, IL-12, TNF, and TIMP-1), IL-1ra, MIP1 $\alpha$ , and MCP-1 showed consistent changes during the co-incubation (Fig. 2). We found several different modes by which direct MC–DC contact can modulate cytokine responses. IL-1ra secretion by DCs is significantly up-regulated only when DCs were allowed to be in direct contact with actMCs (Fig. 2, left, compare DC with DC+actMC). On the other hand, MCP-1 secreted by actMCs was down-regulated when MCs and DCs were not in contact, but direct MC–DC interaction prevented this down-regulation (Fig. 2, top right, compare DC+actMC with DC+actMC\_TW). MIP $\alpha$  secretion by actMCs was down-regulated in the presence of DCs, but direct MC–DC interaction delayed this down-regulation (Fig. 2, center, compare 2 h and 12 h DC+actMC). We note that TNF consistently increased with activation of MCs as expected (Fig. 2, bottom, right graph). These data indicate that cytokine production by MCs and DCs is differentially regulated depending on whether direct cellular interaction occurs. We postulate that the formation of cell–cell contacts alters cell signaling, likely through activation of adhesion molecules, and leads to changes in the quality and the timing of the cytokine response.

### MC–DC interactions depend on MC activation and induce MC polarization

The IHC experiments suggest the potential for direct contact between MCs and DCs *in vivo*, whereas the cytokine measurements show that direct contact alters the cellular response. However, the nature and dynamics of these cellular interactions remained to be determined. We, therefore, performed *in vitro* microscopy to examine the spatiotemporal relationship of the direct MC–DC interaction. In these experiments, imDCs were plated first and allowed to adhere to the coverslip. Then, MCs that were primed with fluorescently labeled  $\alpha$ -DNP IgE were washed and added to the chamber to be monitored over time (Fig. 3 A). MCs were activated by addition of DNP-BSA. Cross-linking of IgE-bound Fc $\epsilon$ RI stimulates multiple signaling pathways (Gilfillan and Tkaczyk, 2006; Yamashita et al., 2007) and, ultimately, results in endocytosis of the receptors.

In the unactivated state, the MCs primarily remain in suspension, and interactions with imDCs are short lived (Fig. 3 A, top row; and Video 1). Activation of MCs resulted in longer lived MC–DC contacts (Fig. 3 A, bottom row; and Videos 2 and 3). Fig. 3 B demonstrates the increase in duration of MC–DC inter-

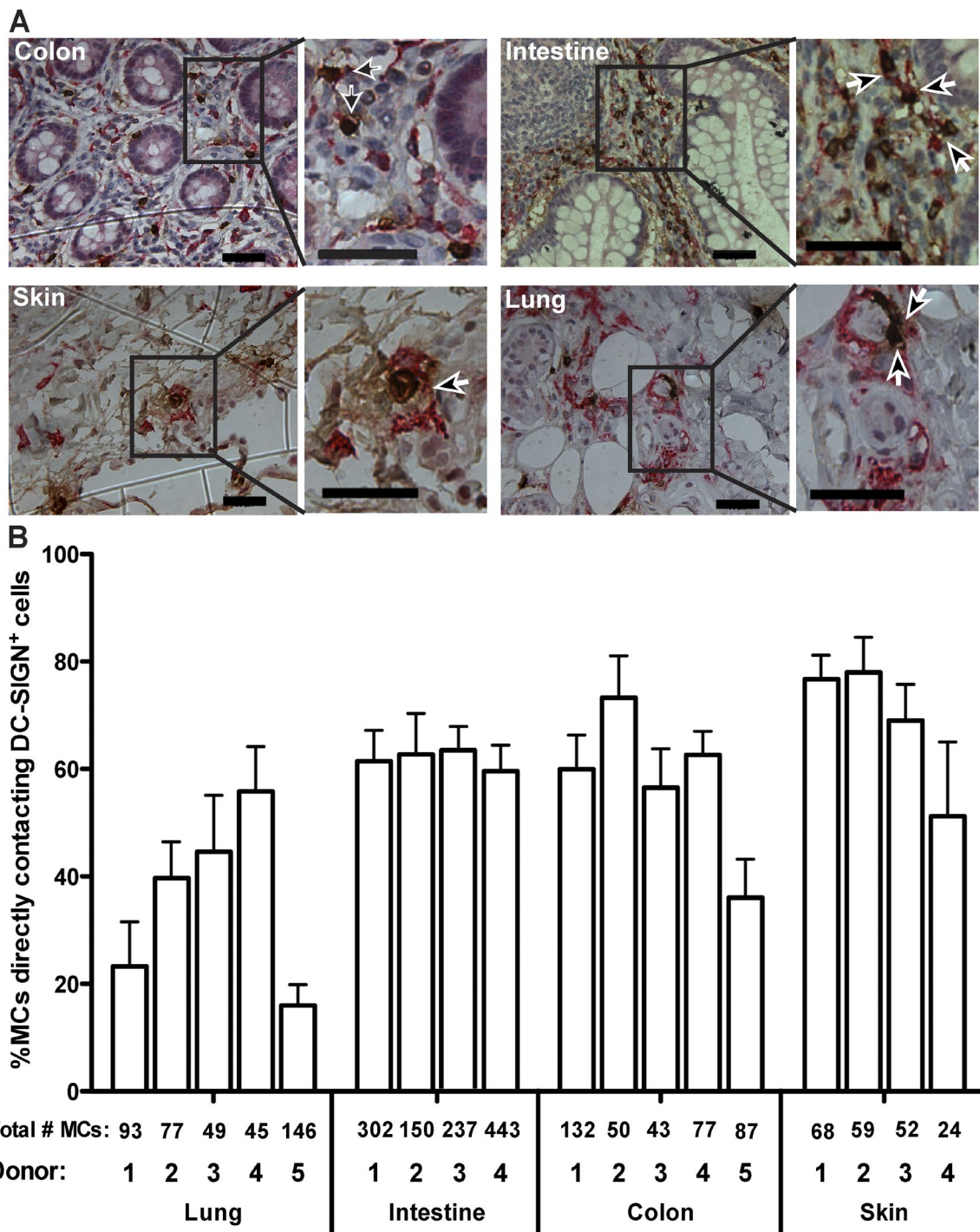


**Figure 1. MCs and DCs are found in close proximity in human tissue.** (A) Representative immunohistochemical labeling of MCs (tryptase, brown) and DCs (DC-SIGN, pink) in 5- $\mu$ m-thick tissue sections from human donors for normal colon, small intestine, lung, and skin. Boxed regions are enlarged to demonstrate where cells are likely in contact (brown and pink pixels are immediately adjacent, indicated by arrows). Images are brightness and contrast enhanced. Bars, 50  $\mu$ m. (B) Bar graph indicating the percentage of MCs in contact with DCs within each type of tissue from each donor tested. Values are means from 10 fields of view for each tissue from each donor. Total numbers of MCs counted for each donor—used to calculate the percentages—are immediately below the bar they represent. Error bars are SEM.

actions when MCs are activated. Examination of MC-DC behavior in Video 1 showed only brief interactions, with 27 MC-DC contacts ranging in duration from 4–48 s (mean of  $11 \pm 1.8$  s). In comparison, actMC-DC interactions in Video 2 persisted as long as 490 s (mean of  $243 \pm 68.3$  s), with many contacts continuing beyond the time series (Fig. 3 B). A typical example of act-

MCs behavior in the presence of imDCs can be seen in Fig. 3 A (bottom row; and Video 3), where an actMC (labeled with Alexa Fluor [AF] 488-IgE, green) maintains contact with a DC for >3 min. The cell-cell interactions were often accompanied by an accumulation of fluorescent IgE at the contact site (Fig. 3 A, bottom row). This behavior was consistently observed across many inde-

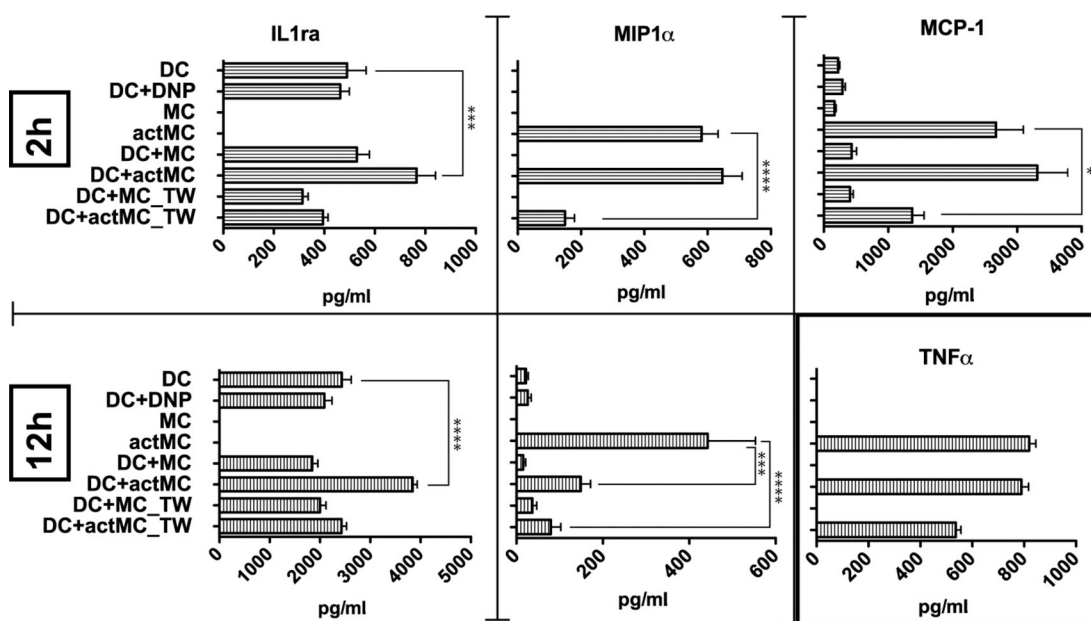


**Figure 2. DC interactions with actMCs alter cytokine secretion.** ELISA results for supernatants from BMMC-imDC experiments at 2 and/or 12 h comparing secretion of IL-1 $\alpha$ , MIP-1 $\alpha$ , MCP-1, and TNF under different conditions were plotted. Results are representative of data from  $\geq 3$  independent experiments for each cytokine tested. Samples are as follows: DC, DCs alone; DC+DNP, DCs with DNP-BSA; MC, MC alone; actMC, MCs activated with DNP-BSA; DC+MC, co-culture of MC and DCs; DC+actMC, co-culture of DNP-BSA activated MCs and DCs; DC+MC\_TW, DCs and MCs separated by a transwell; and DC+actMC\_TW, activated MCs separated from DCs by a transwell. Bonferroni's multiple comparison tests were performed to determine significance. P-value is relative to the number of asterisks (\*, P < 0.01; \*\*, P < 0.001; \*\*\*, P < 0.0001). For IL-1 $\alpha$ , changes are compared with DC sample and for MIP-1 $\alpha$ , and MCP-1 changes are compared with actMC sample. (bottom right) TNF secretion shows the expected increase with MC activation and is not altered by DC interactions. Error bars are SEM.

pendent experiments ( $n = 3$ –20 independent preparations) using three types of MCs: bone marrow–derived MC (BMMC), peritoneal-derived MC (PMC), and the MC/9 cell line (Fig. S2). It is interesting to note that although the MC/9 cell line did not respond to cross-linking with the typical release of granular contents (no measurable  $\beta$ -hexosaminidase release; unpublished data), the vesicle accumulation and enhanced cell–cell contacts were similar to BMMCs and PMCs. In addition, the MC/9 cells formed a uropod-like structure upon activation that was readily observed in 13% of the cells imaged (173 cells analyzed; Video 4).

To confirm that the observed cell–cell contacts were a result of changes in MC–DC interaction strength, we directly measured the adhesion force between the cell types using single cell force spectroscopy. In these experiments, imDCs were plated on the coverslip surface and a tipless atomic force microscopy (AFM) cantilever coated with concanavalin A was used to pick up individual MCs and bring them into contact with a single imDC adhering to the coverslip (Fig. 3 C and Fig. S3). After 5 s of contact, the MC/9 cell was withdrawn and the force necessary to separate the cells was measured. The detachment force necessary to separate actMCs from imDCs is approximately twofold higher compared with unactivated MCs (Fig. 3, D and E; and Fig. S3). Similar force measurements between actMCs and fibroblasts (Fig. 3 E) showed no enhanced interaction, confirming that the interactions between actMCs and DCs are specific. These results are consistent with the more prolonged interactions observed by confocal microscopy (Fig. 3, A and B) and suggest a role for adhesion molecules in facilitating the MC–DC interactions.

The observations that, in the presence of imDCs, MC endosomes are less dispersed and appear to accumulate at the

contact site (Fig. 4 A) suggested “polarization” of the MCs and formation of a cellular synapse. We confirmed that the aggregated receptor was internalized by incubating the cells with low pH buffer (Fig. S4). Exposure to low pH buffer, or “acid stripping,” will remove surface exposed IgE. Because acid stripping did not remove the accumulation of IgE–Fc $\epsilon$ RI, these structures are internalized vesicles, as expected with cross-linked IgE–Fc $\epsilon$ RI (Wilson et al., 2004; Fattakhova et al., 2006; Cleyrat et al., 2013). To determine whether the actMCs are indeed polarized during their interactions with the imDCs, we examined their cytoskeletal reorganization in relation to the cell–cell contact site. For these experiments, MCs were activated in the presence of imDCs, and samples were fixed and stained for actin and tubulin (Fig. 4 B). We consistently observed the localization of the microtubule-organizing center (MTOC) proximal to the largest accumulation of IgE-containing vesicles, confirming that the MCs become polarized upon engagement with imDCs. This polarization (defined as the presence of IgE-containing vesicle aggregation that is also aligned with the MTOC) was observed in 58% of the actMCs, as calculated from the fixed MC–DC samples. A decrease in F-actin is also observed when the polarized endosomes are close to the membrane (Fig. 4 B). The MTOC alignment and displacement of actin are maintained even after MC–DC contact is lost (Fig. S5). Alignment of the MTOC and rearrangement of actin are both consistent with the cytoskeletal architecture reported for T cell–DC synapses (Martín-Cófreces et al., 2011; Smoligovets et al., 2012; Angus and Griffiths, 2013). Collectively, these results indicate that MCs and DCs interact through formation of a synapse that is regulated by MC activation.

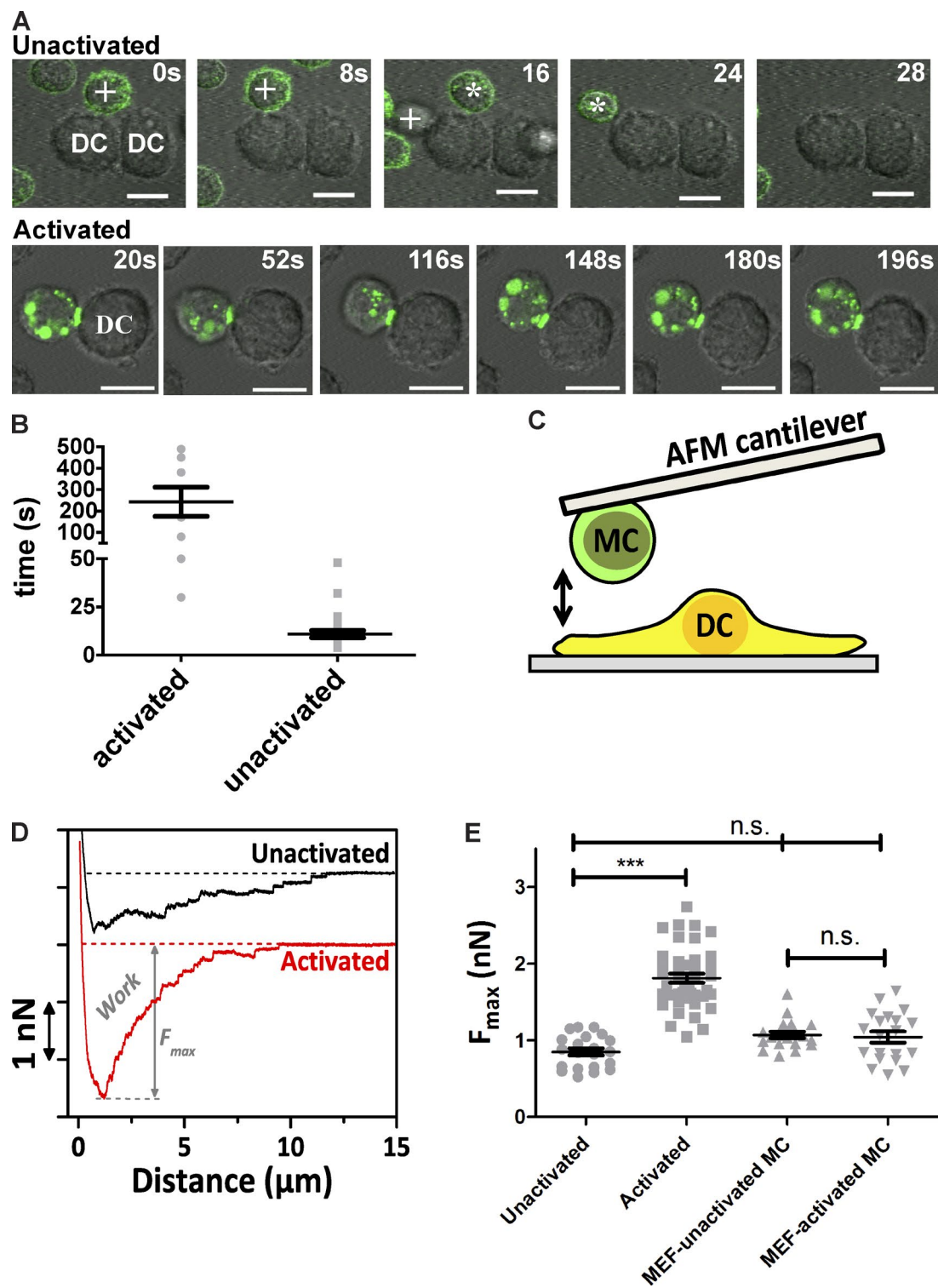


**Figure 3. Activation of MCs in the presence of imDCs leads to increased MC-DC interactions.** (A) Typical interaction between either resting (top row) or activated (bottom row) BMMCs and imDCs. (top row) Movements of two separate unactivated BMMCs (represented by either asterisks or plus signs) are tracked along a DC. (bottom row) ActMCs can maintain contact with imDCs for extended periods and demonstrate polarized accumulation of IgE (AF488, green). (B) Duration of MC-DC interactions observed in Video 1 (unactivated, 27 contacts) and Video 2 (activated, 9 contacts). (C) Cartoon demonstrating the single-cell adhesion measurement setup where MCs are first attached to a tipless AFM cantilever then brought into contact with the imDC. (D) Single representative force-distance (F-D) curves of the interaction of an unactivated versus activated MC (MC/9) interacting with an imDC out of five independent experiments. In total,  $n > 21$  MC-DC contacts and  $n > 120$  F-D curves per condition were measured. From these single curves, the work [area under the curve] and  $F_{max}$  (maximum force to baseline) are quantified. (E) The force in nanonewtons needed to detach unactivated or activated MC/9 MCs from imDCs (unactivated:  $n = 21$  DC-MC contacts in five experiments; activated:  $n = 43$  DC-MC contacts in six experiments) or mouse embryonic fibroblasts (MEF; unactivated:  $n = 19$  DC-MC contacts in two experiments; activated:  $n = 20$  contacts in two experiments). \*\*\*,  $P < 0.001$  (by Mann-Whitney test). Values are means  $\pm$  SEM.

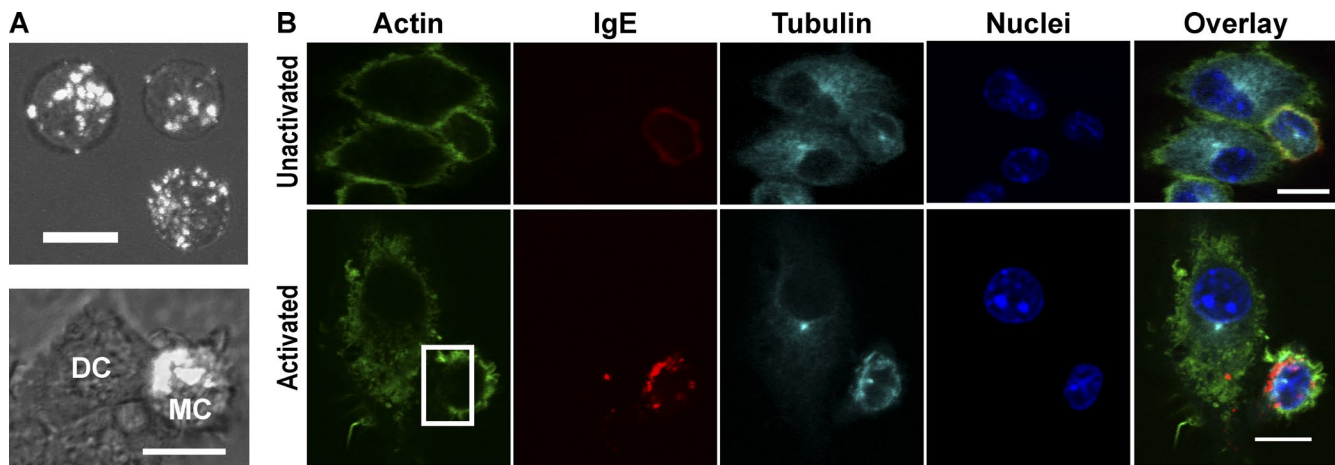


**Figure 4. ActMCs polarize when in the presence of imDCs.** (A) Maximum projection images of BMMCs primed with fluorescent  $\alpha$ -DNP IgE (white) and activated with DNP-BSA. Internalized, cross-linked IgE-Fc $\epsilon$ RI of activated BMMCs alone is dispersed throughout the cell (top); however, direct contact of activated BMMCs with imDCs results in accumulation of IgE-containing vesicles (bottom). Overlays are differential interference contrast from single Z-slice of same cells. (B) Single planes of confocal Z-stack images of fixed cell labeling of either unactivated (top row) or activated (bottom row) BMMC-DC interactions. ActMCs demonstrate depletion of actin at the site of endosome aggregation near the membrane (box, Activated, actin image), as well as positioning of the MTOC to the side of endosome aggregation (Activated, tubulin image). 58% of actMCs show the polarized phenotype, i.e., demonstrate accumulation of endosomes proximal to the MTOC (33 cells counted across three independent experiments). All images are brightness and contrast enhanced. Bars, 10  $\mu$ m.

#### Synapse formation facilitates intercellular transfer of MC antigen

In addition to stimulation of signaling pathways for immune modulation, synapses between immune cells have been reported to provide a mechanism of material transfer between cells (Martín-Cófreces et al., 2011; Angus and Griffiths, 2013; Choudhuri et al., 2014). We observed that direct contact between actMCs and imDCs results in transfer of endocytosed AF555-IgE-Fc $\epsilon$ RI from the MC to the DC (Fig. 5 A). Material transfer was observed in 80% of DCs analyzed from fixed actMC-imDC samples. This material transfer was rapid, occurring within 30 min of MC activation. Direct contact was required for material transfer, as transfer was not detected in DCs that were separated from actMCs by a transwell (unpublished data). To characterize the mechanism of material transfer, we transfected MCs with glycosylphosphatidylinositol (GPI)-GFP (a membrane marker) or CD9-GFP (an exosome marker) and examined material transfer from actMCs to imDCs. Although cells expressing GPI-GFP transferred endosomal contents as expected, these complexes did not contain GPI-GFP (Fig. 5 B, top; and Video 5). CD9-GFP, on the other hand, colocalized with the polarized vesicles and cotransferred with fluorescent IgE to imDCs (Fig. 5 B, bottom; and Video 6). The transferred MC endosomal contents in imDCs also colocalized with the early endosomal marker, EEA1, indicating that transferred material moves through the DC endosomal pathway at least to some extent (Fig. 5 C).

#### Synapse formation and intercellular antigen transfer depend on integrin engagement

Fc $\epsilon$ RI activation has been shown to up-regulate VLA-4 affinity in MCs (Hernandez-Hansen et al., 2004), and VLA-4 and LFA-1 have been shown to be important in a variety of contacts between different immune cell types as well as to modulate MC-DC intercellular communication (Chigaev et al., 2007; Sadhu et al., 2007; Dudeck et al., 2010; Otsuka et al., 2011; Springer and Dustin, 2012). However, it is still not known whether integrins are required for MC-DC interactions or material transfer.

We disrupted integrin activity by preincubation of MCs with the small molecule inhibitors LDV (VLA-4) or Zyn (LFA-1; Chigaev et al., 2011a,b). LDV was derived from the LDV sequence within the VLA-4-binding region of fibrinogen and has been shown to block interaction with VCAM-1 (Chigaev et al., 2001), whereas Zyn is an  $\alpha/\beta$  I-like allosteric  $\beta$ 2 integrin antagonist compound (Shimaoka and Springer, 2003; Chigaev et al., 2015). Although inhibitor treatment was not sufficient to completely abrogate cell contacts, MC polarization was dramatically reduced from 58% to 6.7% with LFA-1 inhibition and to 16% with VLA-4 inhibition (Fig. 6 A). Consistent with this, the small molecule inhibitors also reduced the number of DCs containing transferred material, from 80% of DCs showing material transfer in untreated samples to 46% and 33% showing transfer with Zyn or LDV treatment, respectively (Fig. 6 A). The requirement for integrin engagement for synapse stability was further demonstrated by single-cell force spectroscopy measurements. In the presence of either the small molecule inhibitors or an antibody cocktail that blocks VLA-4 and LFA-1 binding, adhesion between the cells was decreased to levels similar for unactivated MCs and imDCs (Fig. 6 B). We also treated cells with the Src Family kinase inhibitor PP2. PP2 prevents Fc $\epsilon$ RI phosphorylation and, therefore, any downstream signaling that would up-regulate integrin affinity, but it does not interfere with receptor cross-linking or internalization (Andrews et al., 2008). Pretreatment with PP2 completely blocked the increase in cell-cell adhesion when MCs were activated (Fig. 6 B). These results demonstrate that cell adhesion mediated by integrins is important for the efficient formation of the MC-DC synapse. To test whether integrins simply act to mediate cell-cell contact, we subjected MC-DCs to centrifugation to force cell-cell proximity/interaction. In this assay, MC activation also lead to an increase in material transfer ( $27.4 \pm 5.7\%$  with actMCs compared with  $10.4 \pm 4.3\%$  with unactivated MCs). We note the increased background of material transfer when compared with the experiments with DCs plated on glass in which transfer was not observed for unactivated MCs. Inhibition of VLA-4 by LDV

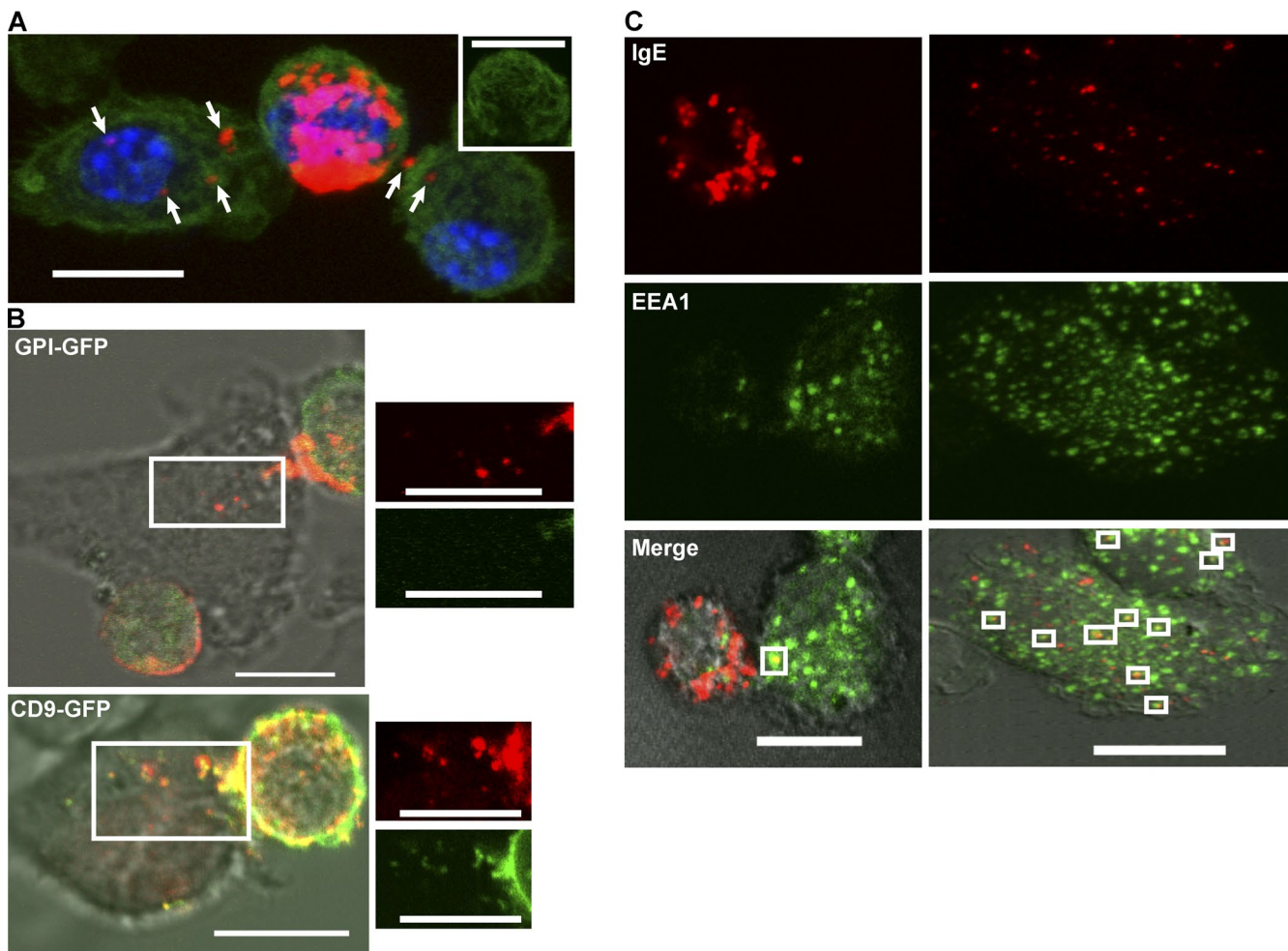


**Figure 5. Activated MCs transfer internalized IgE-Fc $\epsilon$ RI to DCs through direct contact.** (A) Maximum projection image from a confocal Z stack of a typical example of material transfer between an activated BMMC labeled with AF555-IgE (red) in contact with two immature BMDCs (seen in 36 of 45 cells counted across three independent experiments). Cells are fixed and labeled for actin (green) and nuclei (blue). Arrows indicate multiple occurrences of material transfer to each DC. The inset shows the actin labeling for the actMC, demonstrating actin clearance at the site of IgE-Fc $\epsilon$ RI accumulation. Image contrast in the red channel is enhanced to visualize the material transfer (puncta in the DCs) that is much lower in intensity than the MC-localized IgE. (B, top) The membrane marker GPI-GFP (green) transiently expressed in transfected BMMCs does not transfer to imDCs with the IgE-containing vesicles (red puncta). (bottom) When transiently expressed in transfected BMMCs, the endosomal marker, CD9 (green) does colocalize with the IgE-containing vesicles (red), both within the MCs and in those that have been transferred to the imDCs. White, boxed regions are enlarged and channel separated to the right of each merged image. Consistent results were acquired from two independent transfection experiments for each marker. (C) Representative images (from six independent experiments) of fixed labeling of actMCs co-incubated with imDCs. Cells were fixed after the indicated time and demonstrate colocalization of transferred material (IgE, red) with early endosomal compartments (EEA1, green), in the DCs (white boxes in merged image). The 10-min images (left) show an actMC in contact with a DC. The 30-min images (right) do not contain a MC, presumably because the interaction was lost by 30 min. All images were brightness and contrast enhanced. Bars, 10  $\mu$ m.

treatment still blocked material transfer ( $6.9 \pm 3.4\%$ ) even when MCs and DCs were forcibly conjugated through centrifugation, demonstrating that signaling through integrins is required for efficient material transfer between MCs and DCs.

#### MC transfer of antigen to DCs leads to T cell activation

A key function of DCs is to capture antigen in peripheral tissues, process it, and then migrate to draining lymph nodes for presentation to T cells, leading to activation of the T cell response. Because we have now observed that antigen captured by MCs can be transferred to imDCs via direct intercellular contact, we sought to determine whether the transferred antigen is processed and presented by DCs. One indication of antigen presentation by DCs is their ability to activate T cells. OTII mice are a well-established model system in which the T cells

express receptors specific to ovalbumin (OVA) peptide (Barden et al., 1998). Using DNP-OVA to activate MCs provides a system to assess whether MC-DC material transfer results in DC antigen processing leading to T cell activation.

First,  $\alpha$ -DNP-IgE-primed MC/9 MCs were activated by DNP-OVA cross-linker for 15 min, washed to remove unbound DNP-OVA, and added to imDCs. After 1 h of actMC-imDC preincubation, OTII T cells were added to the co-culture. For these experiments, 100 ng/ml *Escherichia coli* lipopolysaccharide (LPS) was added concurrently with T cells to facilitate DC maturation and T cell co-stimulation. The level of CD25 (IL2 receptor,  $\alpha$  subunit) was quantified with flow cytometry to measure the level of T cell activation (Fig. 7; Depper et al., 1985). At 16 h after co-culture, the T cells displayed a significant up-regulation of CD25 when in the presence of OVA-DNP actMCs and DCs (Fig. 7 E, 27.9%). This up-regulation is dependent on

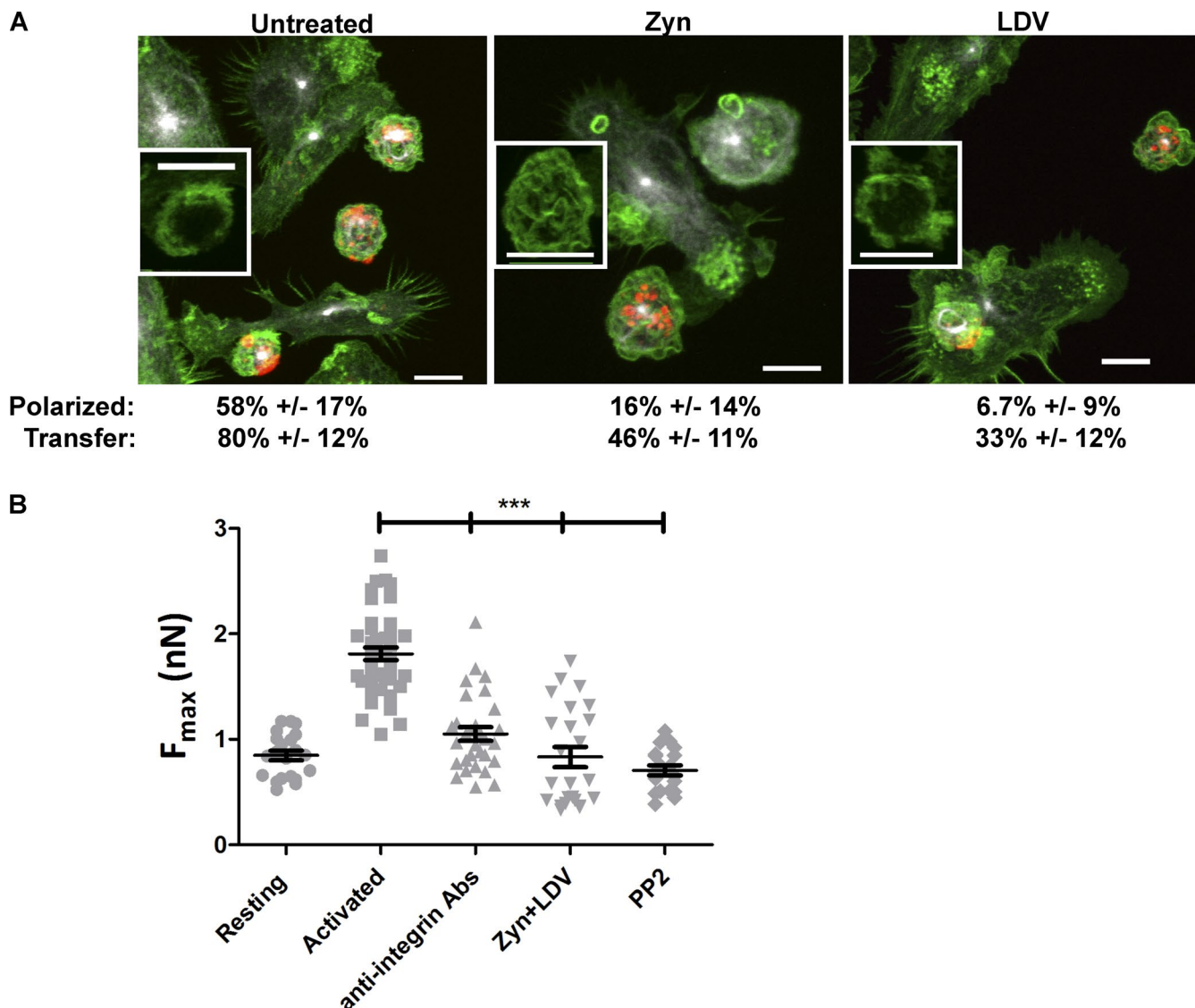


**Figure 6. MC-DC synapse formation requires integrin engagement.** (A) Representative images of functional blocking with small molecule inhibitors for VLA-4 (LDV) and/or LFA-1 (Zyn) disrupts trafficking and polarization of actMC endosomes. Tubulin, white; IgE-Fc $\epsilon$ RI, red; actin, green. Insets are of actin staining (for the MC located below and to the right of each inset) to demonstrate when actin clearance occurred. Values below images indicate the percentages of BMMC demonstrating polarization or the percentages of imDCs demonstrating material transfer (error is the 95% confidence interval). All images are brightness and contrast enhanced. Bars, 10  $\mu$ m. (B) The force in nanonewtons needed to detach actMCs from imDCs under different integrin blocking conditions (Unactivated:  $n = 21$  DC-MC contacts in five experiments; activated:  $n = 43$  contacts in six experiments; anti-integrin antibodies [Abs]:  $n = 30$  contacts in two experiments; Zyn+LDV:  $n = 24$  contacts in three experiments; PP2:  $n = 19$  contacts in two experiments). \*\*\*,  $P < 0.001$  (by Mann-Whitney test). Error bars are SEM.

antigen concentration, as a 10-fold decrease in concentration of OVA-DNP results in decreased CD25 up-regulation (Fig. 7 F, 7.2%). CD25 up-regulation was not seen in the absence of MC activation (Fig. 7 A, 1.9%) or when addition of only the supernatant from the actMC wash was added (Fig. 7 B, 1%). Furthermore, activation of MCs by DNP-BSA, which leads to MC polarization and material transfer (Fig. 4 and Fig. 5), did not induce CD25 up-regulation in OTII T cells (Fig. 7 D, 1.7%), confirming that up-regulation is antigen specific and not merely caused by cytokine release. There are studies that in vitro actMCs can express major histocompatibility class II (Grabbe et al., 1997; Kambayashi et al., 2009) and that direct interactions occur between MCs and T cells (Hershko and Rivera, 2010; Mekori and Hershko, 2012). However, DNP-OVA activation of MCs followed by direct co-incubation with OTII T cells (no

DCs present) did not lead to detectable CD25 up-regulation (Fig. 7 C, 0.4%), consistent with the lack of costimulatory molecules on MCs needed to activate naive T cells directly (Kambayashi et al., 2009). These results demonstrate that material taken up by actMCs and subsequently transferred to DCs can then be processed by the DCs and presented to T cells, leading to productive T cell activation.

## Discussion

Although MC regulation of DC function, especially in the context of bacterial pathogens, has been well studied (Caron et al., 2001a,b; Skokos et al., 2003; Jawdat et al., 2004; Mazzoni et al., 2006; Suto et al., 2006; Shelburne et al., 2009; Dawicki et al.,

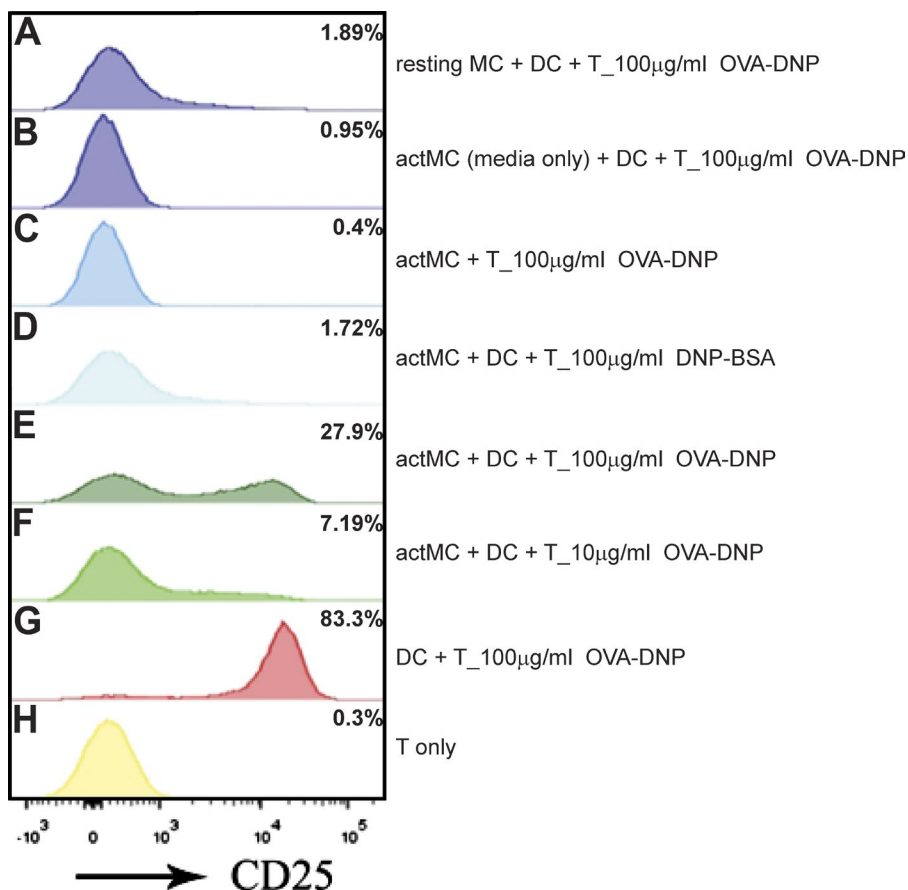


**Figure 7. MC transfer of OVA antigen to DCs results in T cell activation.** MC/9 MCs were activated and incubated with DCs to facilitate antigen transfer. After 1 h of transfer, cells were spun down and co-cultured with 100 ng/ml LPS and T cells for 16 h. Cells were harvested and analyzed using flow cytometry. T cells ( $\text{IgE}^-/\text{CD11c}^+/\text{CD3}^+/\text{CD4}^+$ ) were assessed for CD25 up-regulation. (A) T cells co-cultured with MCs not primed with IgE but in the presence of DNP-OVA and DCs. (B) T cells co-cultured with DCs in the presence of media from IgE-DNP-OVA-activated MCs (no MCs present). (C) T cells co-cultured with IgE-DNP-OVA-activated MCs. (D) T cells co-cultured with DNP-BSA-activated MCs and DCs. (E) T cells co-cultured with 100  $\mu\text{g}/\text{ml}$  DNP-OVA-activated MCs and DCs. (F) T cells co-cultured with 10  $\mu\text{g}/\text{ml}$  DNP-OVA-activated MCs and DCs. (G) T cells activated by DCs directly presenting OVA antigen. (H) T cells alone. Shown is one representative experiment of two.

2010; Reuter et al., 2010; de Vries et al., 2011; Dudeck et al., 2011), the potential significance of direct contact between MCs and DCs is less understood. Here, we demonstrate that these intimate interactions occur throughout the tissues of the body and likely play a role in development of immune responses. Furthermore, we describe two physiological consequences of the MC–DC synapse: modulation of cytokine production and the transfer of antigens to DCs for subsequent T cell activation.

Although phenotypic changes were not visible during in vitro co-incubation of unactivated MCs and imDCs, activation of IgE-primed MCs through Fc $\epsilon$ RI cross-linking resulted in MC polarization with subsequent transfer of MC internalized material to DCs, all of which is contact dependent and requires integrin engagement. Cellular polarization is a hallmark of immune synapses and includes receptor and cytoskeletal reorganization (Dustin et al., 2010; Angus and Griffiths, 2013; Xie et al., 2013), both seen in the actMC–imDC synapse. Specifically, the polarization of IgE-containing endosomes within activated MCs and subsequent material transfer phenotypically resembles delivery of secretory granules in the cytotoxic T-lymphocyte immunological synapse (Xie et al., 2013). Recent evidence has also shown that exosome delivery of major histocompatibility molecules from T cells to B cells facilitates B cell signaling (Choudhuri et al., 2014). Thus, direct synapse facilitated transfer of cellular material—including actMC–imDC interactions shown in our study—may be a generalized mechanism to regulate immune responses.

Consistent with synapse formation, we also showed that MC–DC interactions became longer lived upon MC activation. This prolonged contact was caused by stronger cell–cell interac-

tions and required integrin activity, as confirmed by single-cell force spectroscopy measurements. Integrins are key to many cellular interactions including those formed between immune cells. For example, T cell–DC synapses (Hosseini et al., 2009; Springer and Dustin, 2012), NK target cell adhesion (Hoffmann et al., 2011), and DC–neutrophil interactions (van Gisbergen et al., 2005b) have all been shown to be dependent on integrins. The force needed to detach MCs from DC after 5 s of contact increased from ~1 nN to ~2 nN when MCs were activated and inhibition of integrins decreased the force to unactivated levels. Our interaction values agree well with those found in other integrin-dependent cell–cell interactions. Similar interaction strengths of ~1 nN were found for B cell–T cell contacts in the absence of antigen (Hosseini et al., 2009), and background interaction values of ~1 nN were found for NK cells binding to cells not expressing the adhesion molecule CD48 (Hoffmann et al., 2011). When CD48 was expressed, the interaction strength increased to ~3 nN within 2 min of contact (Hoffmann et al., 2011). B cell–T cell interaction strength increased with even more time: at 15 min T–B cell interaction strength was 4 nN and reached a maximum of ~14 nN after 30 min (Hosseini et al., 2009). We note that actMC and imDC have the ability to form tighter adhesion more rapidly than the other cell systems because we saw increased adhesion after only 5 s. The rapid increase in interaction force between actMC–imDC may be caused by the preactivation of the MC, which has been shown to up-regulate integrin affinity, before interaction with DC. This is in contrast to B, T, or NK target cell interactions in which the binding of adhesion molecules depends on an activation signal. The increased adhesion strength of actMCs was not observed

when interacting with fibroblast cells, confirming that the interactions between actMCs and DCs are specific. Collectively, these data show that integrin signaling is a common pathway used by immune cells to mediate cell–cell communication.

Although the exact mechanism of antigen transfer to DCs remains to be determined, we have shown that it is not merely through trorgocytosis. Within minutes of cross-linking, antigen–IgE–Fc $\epsilon$ RI complexes are rapidly removed from the plasma membrane (Wilson et al., 2004; Fattakhova et al., 2006; Cleyrat et al., 2013). Furthermore, expression of the membrane marker, GFP-GPI, showed that actMC plasma membrane was not transferred with the antigen-containing vesicles. On the other hand, we did observe high colocalization of the exosome marker, CD9-GFP, with IgE-endosomal material, both in MCs and after transfer to DCs. It is therefore tempting to hypothesize that material transfer occurs through an exosome-dependent mechanism. The material transfer between actMCs and imDCs requires direct contact to occur between the two cell types. When separated by a transwell, actMCs are not polarized, and antigen-bearing IgE is not found in DCs. Additionally, disruption of integrins VLA-4 or LFA-1 by small molecule inhibitors reduced MC polarization and material transfer. We also demonstrated that integrin signaling plays a role in material transfer because integrin inhibition reduced MC–DC material transfer even when MC–DC contacts were forced by centrifugation. The BMMCs in these experiments were neither incubated with nor do they express IL-4, a cytokine associated with constitutive secretion of exosomes (Dustin et al., 2010; Angus and Griffiths, 2013), which indicates that the specific actMC–imDC interaction is responsible for triggering material transfer. Polarization of internalized material at the contact site also appears to orient material transfer, as seen in Video 6, where transfer occurs rapidly at the actMC–imDC synapse. Transferred material is found within DC endosomal compartments as indicated by colocalization with the early endosomal marker, EEA1. Although it is IgE that is fluorescently labeled and visualized in our experiments, it is likely that the entire antigen–IgE–Fc $\epsilon$ RI complex is transferred. Previous work has demonstrated that IgE remains associated with the Fc $\epsilon$ RI  $\alpha$ -subunit to well within the lysosomal pathway (Clark and Brugge, 1995).

Finally, we have demonstrated that actMC–imDC synapse formation can regulate the immune response at two levels. First, examination of cytokine production in response to direct contact between imDCs and actMCs demonstrated that direct contact alters secretion of certain cytokines, namely IL-1 $\alpha$ , MCP-1, and MIP-1 $\alpha$ . Soluble mediators are the primary output of MCs upon Fc $\epsilon$ RI cross-linking, many of which affect DC function (Mazzoni et al., 2006; Suto et al., 2006; Shelburne et al., 2009). In previous studies demonstrating influence of actMC byproducts on DCs, bacterial stimulants such as lipopolysaccharide were used in conjunction with Fc $\epsilon$ RI cross-linking antigen to activate MCs, thus resulting in increased production of inflammatory mediators. In our cytokine assays, MC secretion of TNF consistently increased upon activation, demonstrating that MC degranulation was occurring normally under all conditions. Therefore, our observed changes in cytokine production are in response to MC–DC contact rather than altered degranulation. Second, antigen transfer from actMCs to imDCs has a functional consequence: DCs can process and present antigen originally taken up by MCs, leading to T cell activation. Although our assays use a saturating concentration of IgE recognizing a single antigen, in vivo MCs are decorated with a variety of antigen-specific IgE

molecules. Internalization and polarization of a subset of the IgE-bound receptors upon antigen recognition, with subsequent transfer of antigen from MCs to neighboring imDCs, represents a mechanism to enhance the ability of DCs to acquire and present the particular activating antigen. Our data suggest a novel method of antigen sampling *in vivo* via MC uptake of antigen and transfer to DCs for subsequent activation of T cells and may represent a mechanism of propagating MC-centric pathological conditions such as asthma and allergy. Further insights into the mechanisms and outcomes of intercellular crosstalk will be critical to our understanding of the immune response.

## Materials and methods

### Animals and cells

8-wk-old female C57/BL6 mice were purchased from The Jackson Laboratory and used for purification of BMMCs and bone marrow–derived DCs (BMDCs) following approved protocols. OTII transgenic animals were also obtained from The Jackson Laboratory. Cells were derived from the femurs as previously described (Kawakami et al., 2006). In brief, bone marrow was flushed from femurs with either BMMC media (RPMI 1640, 20% FCS, 2 mM L-glutamine, 0.1 mM MEM nonessential amino acids, penicillin/streptomycin, 50  $\mu$ M  $\beta$ -mercaptoethanol, and 10 mM Hepes) or BMDC media (RPMI 1640, 10% FCS, penicillin/streptomycin, 2 mM L-glutamine, and 50  $\mu$ M  $\beta$ -mercaptoethanol). BMMCs were cultivated for 6 wk in BMMC media supplemented with 30 ng/ml recombinant murine IL-3 (Akron Biotech) and 50 ng/ml recombinant murine stem cell factor (PeproTech), and BMDCs were cultivated in BMDC media supplemented with granulocyte macrophage colony-stimulating factor rich supernatant from B7H1-GM Hybridoma cell line (gift from T.M. Laufer, University of Pennsylvania and Philadelphia Veterans Affairs Medical Center, Philadelphia, PA) for 6 d and then used in experiments on days 7–9. MC/9 cells were purchased from ATCC and maintained in recommended media (RPMI 1640, 10% FBS, penicillin/streptomycin, 10% rat T-stim [Thermo Fisher Scientific], 2 mM L-glutamine, and 0.05 mM  $\beta$ -mercaptoethanol). PMCs were derived from the peritoneal cavity of C57/BL6 mice as previously described (Dudeck et al., 2011). In brief, peritoneal lavage was performed with PBS, and cells were cultured in BMMC media supplemented with recombinant murine IL-3 and recombinant murine stem cell factor as described for BMMC. After 2 d, nonadherent cells were carefully removed, and fresh culture medium was added. PMCs were used after 8 d of culture.

### ELISA

BMDCs were plated at  $10^6$  cells/well in 12- and 6-well plates and allowed to adhere overnight. BMMCs were primed with 1  $\mu$ g/ml  $\alpha$ -DNP IgE (Liu et al., 1980) overnight and exchanged to BMDC media (thus removing unbound IgE) at  $10^6$  cells/ml the day of the experiment before addition to BMDCs at 1:1 ratio. MC activation was accomplished with the addition of 0.2  $\mu$ g/ml DNP-BSA (Life Technologies). Supernatants from 2- and 12-h time points were assayed for TNF, IL-12, IL-4, IL-10, IL-13, IL-6 (eBioscience), IL-1 $\alpha$  (R&D Systems), MIP1 $\alpha$  (SABiosciences), TIMP-1 (RayBiotech), PGE2, and MCP-1 (BioLegend).

### IHC

5- $\mu$ m sections of donor tissue mounted onto positive slides were obtained from the Human Tissue Repository at the University of New Mexico following protocol approval. Slides were deparaffinized through three changes of xylene and through graded alcohols to water. Sections were treated with 3% H<sub>2</sub>O<sub>2</sub> to inactivate the endogenous per-

oxidase activity, and antigen retrieval was accomplished by immersing slides in 10 mM citrate solution, pH 6.0, and boiling them for 10 min at 120°C (20–25 p.s.i.) in a Decloaking Chamber (Biocare Medical). Slides were then cooled in buffer for 20 min and rinsed in three changes of deionized water and PBS. Nonspecific binding was minimized by incubating the sections with normal horse serum, in PBS, for 30 min. Labeling of sections was performed using PicTure Double Staining kit (Life Technologies). In brief, sections were incubated overnight at 4°C with primary antibodies for CD209 (rabbit anti-human DC-SIGN; LIFESPAN Biosciences) or MC tryptase (mouse monoclonal anti-human; Dako) and washed. After incubation with the polymer secondary antibodies provided with the kit (goat anti-mouse IgG-HRP polymer conjugate and goat anti-rabbit IgG-AP polymer conjugate), sections were developed with the chromogenic substrates, DAB and Fast Red, rinsed with deionized water and PBS, counterstained with hematoxylin, dehydrated through graded alcohols, and permount with ClearMount (Life Technologies). Imaging was performed on an upright microscope (Axioskop 2 MOT; Carl Zeiss) with a 40× oil objective and digital color camera (AxioCam; Carl Zeiss). Images were acquired with SlideBook Image Acquisition software (3i Intelligent Imaging Innovations) and processed in ImageJ (National Institutes of Health; Abràmoff et al., 2004). Quantitation of contacts was performed by visually assessing the number of MCs (Fig. 1 A, brown) that were immediately adjacent to DC (Fig. 1 A, pink) pixels. 10 fields of view were assessed for each tissue tested, and all MCs were counted to calculate the percentage of MCs in contact with DC.

#### Live-cell imaging and treatment with inhibitors

Conjugation of α-DNP IgE (Liu et al., 1980) to NHS-ester-AF647, 555, or 488 (Life Technologies) was performed at a 1:1 ratio as described in the product manual. BMDCs were seeded into Labtek 8-well chambers (Thermo Fisher Scientific), and BMMCs were preincubated overnight with 1 µg/ml α-DNP IgE. Before assays, BMMCs were pelleted to remove any free IgE and exchanged into BMDC media. Small molecule inhibitors LDV and Zyn were used to block VLA-4 and LFA-1 interactions (respectively, gifted by A. Chigaev, The University of New Mexico, Albuquerque, NM; Morelli et al., 2004; Sadhu et al., 2007). IgE-labeled BMMCs and BMDCs were pretreated with vehicle (DMSO) or 1 µM LDV and/or Zyn for 30 min in BMDC media and combined at a 1:1 ratio, and BMMCs were activated with 0.2 µg/ml DNP-BSA (Life Technologies). Confocal microscopy was performed using a microscope (LSM 510META; Carl Zeiss) with a 63×, 1.2 NA water objective. An objective heater (Bioptrons) was used to maintain sample temperature at ~37°C.

#### AFM adhesion measurements

AFM experiments were performed on a Catalyst BioScope AFM (Bruker) mounted on an inverted microscope (TCS SP5 II; Leica) with a 40×, 0.85 NA air objective at 37°C. Images were taken with a brightfield camera (ORCA-05G; Hamamatsu Photonics), and data were exported from the BioScope Catalyst by the NanoScope Version 8.15 software and further analyzed in MATLAB (MathWorks). Origin 8.1 (OriginLab) and Prism (GraphPad Software) were used for fitting and statistics. Immature BMDCs were seeded sparsely on a Willco dish and allowed to adhere for ≥12 h before experiments. For experiments, MC/9 cells were incubated with AF555 α-DNP IgE overnight. MC/9 cells were then added to BMDCs in either an unactivated or activated state. For activation, MCs were incubated with 0.2 µg/ml DNP-BSA for 15 min and then washed before addition. A single MC/9 was picked up by gently compressing it between a concanavalin A (Sigma-Aldrich)-coated tipless NP-O (Bruker) AFM cantilever and the glass, applying a ~5-nN contact force. After letting it adhere for 5 min, the

MC/9 cell was brought into contact with flat parts of an imBMDC, applying a 2 nN contact force for 5 s with approach and retract velocities of 10 µm/s. Detachment forces and work were determined after baseline correction of (F-D) curves with a macro in MATLAB (te Riet et al., 2014). Blocking experiments were performed with a mixture of antibodies to LFA-1 (rat monoclonal; Life Technologies) and VLA-4 (rat monoclonal; EMD Millipore), with small molecule inhibitors (as described in live cell imaging) or with the Src-family tyrosine kinase inhibitor PP2 (Life Technologies).

#### Fixed cell immunofluorescence

To visualize the MTOC and actin structure of MCs, fixed immunocytochemistry was performed as follows. BMDCs were seeded onto coverslips, and BMMCs were preincubated with AF555 α-DNP IgE overnight. Before experiments, BMMCs were washed, exchanged to BMDC media, and added to BMDCs at a 1:1 ratio. Activation of samples was accomplished with addition of DNP-BSA for 30 min. All samples were fixed with 4% paraformaldehyde, permeabilized with 0.5% Triton X-100, and labeled with AF488 phalloidin (Life Technologies), DAPI, and α-β-tubulin AF647 (rabbit monoclonal; Cell Signaling Technology). Fixed immunocytochemistry for localization of β3 was performed. BMMCs labeled with AF555 α-DNP IgE were activated and incubated with BMDCs at 37°C, 5% CO<sub>2</sub> for 30 min. Samples were fixed with 4% paraformaldehyde, permeabilized with 0.5% Triton X-100, incubated with α-β3 (goat polyclonal; Santa Cruz Biotechnology, Inc.) followed by incubation with an AF647-conjugated secondary (donkey; Life Technologies). Coverslips were mounted using ProLong Gold (Life Technologies) and imaged with laser-scanning confocal microscopy (LSM 510META; Carl Zeiss) and 63×, 1.4 NA oil objective.

#### Transfection

BMMCs were transfected with either GPI-GFP or CD9-GFP expression plasmids (both are the pEGFP backbone with cytomegalovirus promoter; gifted by J. Gillette, The University of New Mexico, Albuquerque, NM) using the Amaxa Nucleofector (program T-30) and Solution T (Lonza). Transfected cells were allowed to recover for ≥6 h before use in live-cell imaging experiments.

#### Quantitation of material transfer and cellular polarization

To determine DCs that contained material transferred from activated MCs in each condition, confocal Z stacks from at least three independent experiments were assessed for the presence of fluorescent-IgE in DC populations. As transferred material was small and punctate in nature, the channel for IgE label was brightness and contrast enhanced to ensure that these spots were not overlooked. For quantitation of cellular polarization and material transfer, three conditions were examined (untreated, LDV treated, and Zyn treated). MCs were pretreated with 1 µM LDV or 1 µM Zyn for 30 min before addition to DCs. Samples were fixed after activation and stained for microtubules and confocal Z stacks (on ≥10 fields of view for each condition) were assessed. Imaging was performed using a microscope (LSM 510META) with a 63×, 1.4 NA oil objective. Stacks were opened in ImageJ (Abràmoff et al., 2004), converted to maximal intensity Z projections, and analyzed for the presence of IgE accumulation on one side of the cell as well as localization of the MTOC internal to that accumulation. Only cells that demonstrated both characteristics were counted as polarized. The multinomial coefficient and 95% confidence interval for each condition are calculated independently for each treatment (Fig. 4 D).

#### Forced MC-DC interaction assay

MC/9 cells and BMDCs were grown as described. Before the assay, MC/9 cells were incubated with AF488-IgE for 3–4 h and then washed

and transferred to BMDC media at a concentration of  $10^6$  cells/500  $\mu$ l. Samples included unactivated, activated, LDV treated (1  $\mu$ M, 30 min pretreatment), and DMSO control. MCs were activated with 0.2  $\mu$ g/ml DNP-BSA for 10 min. BMDC were removed from plates and kept at a concentration of  $10^6$  cells/500  $\mu$ l. BMDC were then added to MC/9 samples and centrifuged for 3 min at 400 g and then maintained at 37°C for 30 min. At the end of incubation, paraformaldehyde was added to a final concentration of 4% and allowed to incubate for 15 min. Samples were washed with PBS, stained with AF647- $\alpha$ -CD11c (Armenian hamster monoclonal; eBioscience) for 30 min to label DCs, washed again with PBS, and mounted with ProLong Gold (Life Technologies). Confocal imaging was performed (LSM 510META, 63 $\times$ , 1.4 NA oil objective), and the percentage of DCs demonstrating uptake of AF488-IgE was quantitated for all conditions tested with  $\geq 190$  cells counted per sample.

#### T cell activation and proliferation assay

MC/9 cells and BMDCs were generated as described in Animals and cells. For T cell activation, MC/9 cells, incubated overnight with 1  $\mu$ g/ml  $\alpha$ -DNP IgE, were activated with 100  $\mu$ g/ml DNP-OVA for 15 min and subsequently washed three times with fresh media. Washed, activated MC/9 was then co-cultured with BMDCs for 1 h at 37°C, 5% CO<sub>2</sub>. OTII transgenic T cells were isolated from spleen and lymph nodes of OTII Tg animals using the pan-T cell Miltenyi kit (Miltenyi Biotech) and added to MC-DCs along with 100 ng/ml LPS (Sigma-Aldrich). Final cell ratio was 1:2:2 MC/DC/T cell. Cells were harvested at 16 h after co-culture and analyzed using flow cytometry using Fortessa (BD). T cells were identified using IgE AF647, CD11c-PERCPCY5.5 (Armenian hamster monoclonal), CD3-PECY7 (rat monoclonal; BD), and CD4-PECY7 (rat monoclonal; BioLegend) using an IgE<sup>-</sup>CD11c<sup>-</sup>CD3<sup>+</sup>CD4<sup>+</sup> gate. Activated T cells were identified as CD25PE<sup>hi</sup> (eBioscience). Analyses were performed using FlowJo (Tree Star).

#### Online supplemental material

Fig. S1 shows IHC controls. Fig. S2 shows the formation of MC-DC interactions for three types of MCs. Fig. S3 contains further description of the single-cell force spectroscopy experiments. Fig. S4 demonstrates the acid stripping experiment. Fig. S5 contains further examples of MC polarization. Video 1 demonstrates the brief interactions between unactivated MCs and DCs. Videos 2 and 3 show the increased interaction time between actMCs and DCs as well as the aggregation of IgE-containing vesicles to the contact site. Video 4 shows the formation of a uropod by actMC/9 cells. Video 5 shows that GPI-GFP is not transferred during BMMC and DC interactions. In Video 6, cotransfer of CD9-GFP with fluorescent IgE to the DC can be seen. Online supplemental material is available at <http://www.jcb.org/cgi/content/full/jcb.201412074/DC1>. Additional data are available in the JCB Data-Viewer at <http://dx.doi.org/10.1083/jcb.201412074.dv>.

#### Acknowledgements

The authors would like to thank Dr. Alexandre Chigaev for providing the LFA-1 and VLA-4 small molecule inhibitors, Dr. Jennifer Gillette for providing the CD9-GFP and GPI-GFP expression vectors, Dr. Dallas Flies for assistance with BMDC preparation, and Dr. Bridget Wilson for helpful discussion. Images in this paper were generated in the University of New Mexico and Cancer Center Fluorescence Microscopy Shared Resource (funding detail can be found at <http://hsc.unm.edu/crcf/microscopy/acknowledgement.shtml>). AFM experiments were conducted at the Microscope Imaging Center of the Radboud Institute for Molecular Life Sciences. Flow cytometry was performed at The University of New Mexico Cancer Center Flow Cytometry Shared Resource.

This work was supported by a Human Frontiers Science Program Young Investigator Award to D.S. Lidke and A. Cambi (RGY0074/2008), National Institutes of Health grant R01GM100114 to D.S. Lidke, National Institutes of Health grant 5R01AI097202 to J.L. Cannon, and the New Mexico Spatiotemporal Modeling Center grant P50GM085273. A. Cambi is the recipient of a Meervoud grant 836-09-002 and J. te Riet of a Veni grant 680-47-421, both from the Netherlands Organization for Scientific Research (NWO). An NWO Medium Sized Investment NWO-ZonMW 91110007 also supported this research.

The authors declare no competing financial interests.

Submitted: 15 December 2014

Accepted: 17 July 2015

#### References

- Abràmoff, M.D., P.J. Magalhães, and S.J. Ram. 2004. Image processing with ImageJ. *Biophotonics International*. 11:36–42.
- Allam, J.P., G. Stojanovski, N. Friedrichs, W. Peng, T. Bieber, J. Wenzel, and N. Novak. 2008. Distribution of Langerhans cells and mast cells within the human oral mucosa: new application sites of allergens in sublingual immunotherapy? *Allergy*. 63:720–727. <http://dx.doi.org/10.1111/j.1398-9995.2007.01611.x>
- Andrews, N.L., K.A. Lidke, J.R. Pfeiffer, A.R. Burns, B.S. Wilson, J.M. Oliver, and D.S. Lidke. 2008. Actin restricts Fc $\epsilon$ RI diffusion and facilitates antigen-induced receptor immobilization. *Nat. Cell Biol.* 10:955–963. <http://dx.doi.org/10.1038/ncb1755>
- Angus, K.L., and G.M. Griffiths. 2013. Cell polarization and the immunological synapse. *Curr. Opin. Cell Biol.* 25:85–91. <http://dx.doi.org/10.1016/j.ceb.2012.08.013>
- Barnden, M.J., J. Allison, W.R. Heath, and F.R. Carbone. 1998. Defective TCR expression in transgenic mice constructed using cDNA-based  $\alpha$ - and  $\beta$ -chain genes under the control of heterologous regulatory elements. *Immunol. Cell Biol.* 76:34–40. <http://dx.doi.org/10.1046/j.1440-1711.1998.00709.x>
- Bergman, M.P., A. Engering, H.H. Smits, S.J. van Vliet, A.A. van Bodegraven, H.P. Wirth, M.L. Kapsenberg, C.M. Vandebroucke-Grauls, Y. van Kooyk, and B.J. Appelmelk. 2004. *Helicobacter pylori* modulates the T helper cell 1/T helper cell 2 balance through phase-variable interaction between lipopolysaccharide and DC-SIGN. *J. Exp. Med.* 200:979–990. <http://dx.doi.org/10.1084/jem.20041061>
- Caron, G., Y. Delneste, E. Roelandts, C. Duez, J.Y. Bonnefoy, J. Pestel, and P. Jeannin. 2001a. Histamine polarizes human dendritic cells into Th2 cell-promoting effector dendritic cells. *J. Immunol.* 167:3682–3686. <http://dx.doi.org/10.4049/jimmunol.167.7.3682>
- Caron, G., Y. Delneste, E. Roelandts, C. Duez, N. Herbault, G. Magistrelli, J.Y. Bonnefoy, J. Pestel, and P. Jeannin. 2001b. Histamine induces CD86 expression and chemokine production by human immature dendritic cells. *J. Immunol.* 166:6000–6006. <http://dx.doi.org/10.4049/jimmunol.166.10.6000>
- Carroll-Portillo, A., K. Spendier, J. Pfeiffer, G. Griffiths, H. Li, K.A. Lidke, J.M. Oliver, D.S. Lidke, J.L. Thomas, B.S. Wilson, and J.A. Timlin. 2010. Formation of a mast cell synapse: Fc epsilon RI membrane dynamics upon binding mobile or immobilized ligands on surfaces. *J. Immunol.* 184:1328–1338. <http://dx.doi.org/10.4049/jimmunol.0903071>
- Carroll-Portillo, A., Z. Surviladze, A. Cambi, D.S. Lidke, and B.S. Wilson. 2012. Mast cell synapses and exosomes: membrane contacts for information exchange. *Front. Immunol.* 3:46. <http://dx.doi.org/10.3389/fimmu.2012.00046>
- Chigaev, A., A.M. Blenc, J.V. Braaten, N. Kumaraswamy, C.L. Kepley, R.P. Andrews, J.M. Oliver, B.S. Edwards, E.R. Prossnitz, R.S. Larson, and L.A. Sklar. 2001. Real time analysis of the affinity regulation of  $\alpha$ 4-integrin. The physiologically activated receptor is intermediate in affinity between resting and Mn(2+) or antibody activation. *J. Biol. Chem.* 276:48670–48678. <http://dx.doi.org/10.1074/jbc.M103194200>
- Chigaev, A., A. Waller, G.J. Zwart, T. Buranda, and L.A. Sklar. 2007. Regulation of cell adhesion by affinity and conformational unbending of  $\alpha$ 4 $\beta$ 1 integrin. *J. Immunol.* 178:6828–6839. <http://dx.doi.org/10.4049/jimmunol.178.11.6828>
- Chigaev, A., Y. Smagley, Y. Zhang, A. Waller, M.K. Haynes, O. Amit, W. Wang, R.S. Larson, and L.A. Sklar. 2011a. Real-time analysis of the inside-out regulation of lymphocyte function-associated antigen-1 revealed sim-

ilarities to and differences from very late antigen-4. *J. Biol. Chem.* 286:20375–20386. <http://dx.doi.org/10.1074/jbc.M110.206185>

Chigaev, A., Y. Wu, D.B. Williams, Y. Smagley, and L.A. Sklar. 2011b. Discovery of very late antigen-4 (VLA-4,  $\alpha 4\beta 1$  integrin) allosteric antagonists. *J. Biol. Chem.* 286:5455–5463. <http://dx.doi.org/10.1074/jbc.M110.162636>

Chigaev, A., Y. Smagley, M.K. Haynes, O. Ursu, C.G. Bologa, L. Halip, T. Oprea, A. Waller, M.B. Carter, Y. Zhang, et al. 2015. FRET detection of lymphocyte function-associated antigen-1 conformational extension. *Mol. Biol. Cell.* 26:43–54. <http://dx.doi.org/10.1091/mbc.E14-06-1050>

Choudhuri, K., J. Llodrá, E.W. Roth, J. Tsai, S. Gordo, K.W. Wucherpfennig, L.C. Kam, D.L. Stokes, and M.L. Dustin. 2014. Polarized release of T-cell-receptor-enriched microvesicles at the immunological synapse. *Nature*. 507:118–123. <http://dx.doi.org/10.1038/nature12951>

Clark, E.A., and J.S. Brugge. 1995. Integrins and signal transduction pathways: the road taken. *Science*. 268:233–239. <http://dx.doi.org/10.1126/science.7716514>

Cleynat, C., A. Darehshouri, K.L. Anderson, C. Page, D.S. Lidke, N. Volkmann, D. Hanein, and B.S. Wilson. 2013. The architectural relationship of components controlling mast cell endocytosis. *J. Cell Sci.* 126:4913–4925. <http://dx.doi.org/10.1242/jcs.128876>

Dalod, M., R. Chelbi, B. Malissen, and T. Lawrence. 2014. Dendritic cell maturation: functional specialization through signaling specificity and transcriptional programming. *EMBO J.* 33:1104–1116. <http://dx.doi.org/10.1002/embj.201488027>

Dawicki, W., D.W. Jawdat, N. Xu, and J.S. Marshall. 2010. Mast cells, histamine, and IL-6 regulate the selective influx of dendritic cell subsets into an inflamed lymph node. *J. Immunol.* 184:2116–2123. <http://dx.doi.org/10.4049/jimmunol.0803894>

Depper, J.M., W.J. Leonard, C. Drogula, M. Krönke, T.A. Waldmann, and W.C. Greene. 1985. Interleukin 2 (IL-2) augments transcription of the IL-2 receptor gene. *Proc. Natl. Acad. Sci. USA*. 82:4230–4234. <http://dx.doi.org/10.1073/pnas.82.12.4230>

de Vries, V.C., K. Pino-Lagos, E.C. Nowak, K.A. Bennett, C. Oliva, and R.J. Noelle. 2011. Mast cells condition dendritic cells to mediate allograft tolerance. *Immunity*. 35:550–561. <http://dx.doi.org/10.1016/j.immuni.2011.09.012>

de Witte, L., R.D. de Vries, M. van der Vlist, S. Yüksel, M. Litjens, R.L. de Swart, and T.B. Geijtenbeek. 2008. DC-SIGN and CD150 have distinct roles in transmission of measles virus from dendritic cells to T-lymphocytes. *PLoS Pathog.* 4:e1000049. <http://dx.doi.org/10.1371/journal.ppat.1000049>

Dudeck, A., M. Leist, S. Rubant, A. Zimmermann, J. Dudeck, W.H. Boehncke, and M. Maurer. 2010. Immature mast cells exhibit rolling and adhesion to endothelial cells and subsequent diapedesis triggered by E- and P-selectin, VCAM-1 and PECAM-1. *Exp. Dermatol.* 19:424–434. <http://dx.doi.org/10.1111/j.1600-0625.2010.01073.x>

Dudeck, A., C.A. Suender, S.L. Kostka, E. von Stebut, and M. Maurer. 2011. Mast cells promote Th1 and Th17 responses by modulating dendritic cell maturation and function. *Eur. J. Immunol.* 41:1883–1893. <http://dx.doi.org/10.1002/eji.201040994>

Dustin, M.L., A.K. Chakraborty, and A.S. Shaw. 2010. Understanding the structure and function of the immunological synapse. *Cold Spring Harb. Perspect. Biol.* 2:a002311. <http://dx.doi.org/10.1101/cshperspect.a002311>

Fattakhova, G., M. Masilamani, F. Borrego, A.M. Gilfillan, D.D. Metcalfe, and J.E. Coligan. 2006. The high-affinity immunoglobulin-E receptor (Fc $\epsilon$ RI) is endocytosed by an AP-2/clathrin-independent, dyamin-dependent mechanism. *Traffic*. 7:673–685. <http://dx.doi.org/10.1111/j.1600-0854.2006.00423.x>

Geijtenbeek, T.B., R. Torensma, S.J. van Vliet, G.C. van Duijnhoven, G.J. Adema, Y. van Kooyk, and C.G. Figdor. 2000. Identification of DC-SIGN, a novel dendritic cell-specific ICAM-3 receptor that supports primary immune responses. *Cell*. 100:575–585. [http://dx.doi.org/10.1016/S0092-8674\(00\)80693-5](http://dx.doi.org/10.1016/S0092-8674(00)80693-5)

Gilfillan, A.M., and C. Tkaczyk. 2006. Integrated signalling pathways for mast-cell activation. *Nat. Rev. Immunol.* 6:218–230. <http://dx.doi.org/10.1038/nri1782>

Grabbe, J., L. Karau, P. Welker, A. Ziegler, and B.M. Henz. 1997. Induction of MHC class II antigen expression on human HMC-1 mast cells. *J. Dermatol. Sci.* 16:67–73. [http://dx.doi.org/10.1016/S0923-1811\(97\)00033-9](http://dx.doi.org/10.1016/S0923-1811(97)00033-9)

Hernandez-Hansen, V., A.J. Smith, Z. Surviladze, A. Chigaev, T. Mazel, J. Kalesnikoff, C.A. Lowell, G. Krystal, L.A. Sklar, B.S. Wilson, and J.M. Oliver. 2004. Dysregulated Fc $\epsilon$ RI signaling and altered Fyn and SHIP activities in Lyn-deficient mast cells. *J. Immunol.* 173:100–112. <http://dx.doi.org/10.4049/jimmunol.173.1.100>

Hershko, A.Y., and J. Rivera. 2010. Mast cell and T cell communication; amplification and control of adaptive immunity. *Immunol. Lett.* 128:98–104. <http://dx.doi.org/10.1016/j.imlet.2009.10.013>

Hoffmann, S.C., A. Cohnen, T. Ludwig, and C. Watzl. 2011. 2B4 engagement mediates rapid LFA-1 and actin-dependent NK cell adhesion to tumor cells as measured by single cell force spectroscopy. *J. Immunol.* 186:2757–2764. <http://dx.doi.org/10.4049/jimmunol.1002867>

Hosseini, B.H., I. Louban, D. Djandji, G.H. Wabnitz, J. Deeg, N. Bulbul, Y. Samstag, M. Gunzer, J.P. Spatz, and G.J. Hämerling. 2009. Immune synapse formation determines interaction forces between T cells and antigen-presenting cells measured by atomic force microscopy. *Proc. Natl. Acad. Sci. USA*. 106:17852–17857. <http://dx.doi.org/10.1073/pnas.0905384106>

Jameson, B., F. Baribaud, S. Pöhlmann, D. Ghavimi, F. Mortari, R.W. Doms, and A. Iwasaki. 2002. Expression of DC-SIGN by dendritic cells of intestinal and genital mucosae in humans and rhesus macaques. *J. Virol.* 76:1866–1875. <http://dx.doi.org/10.1128/JVI.76.4.1866-1875.2002>

Jawdat, D.M., E.J. Albert, G. Rowden, I.D. Haidl, and J.S. Marshall. 2004. IgE-mediated mast cell activation induces Langerhans cell migration in vivo. *J. Immunol.* 173:5275–5282. <http://dx.doi.org/10.4049/jimmunol.173.8.5275>

Kambayashi, T., E.J. Allenspach, J.T. Chang, T. Zou, J.E. Shoag, S.L. Reiner, A.J. Caton, and G.A. Koretzky. 2009. Inducible MHC class II expression by mast cells supports effector and regulatory T cell activation. *J. Immunol.* 182:4686–4695. <http://dx.doi.org/10.4049/jimmunol.0803180>

Kawakami, Y., J. Kitaura, and T. Kawakami. 2006. Techniques to study Fc epsilonRI signaling. *Methods Mol. Biol.* 315:175–189.

Kitawaki, T., N. Kadowaki, N. Sugimoto, N. Kambe, T. Hori, Y. Miyachi, T. Nakahata, and T. Uchiyama. 2006. IgE-activated mast cells in combination with pro-inflammatory factors induce Th2-promoting dendritic cells. *Int. Immunol.* 18:1789–1799. <http://dx.doi.org/10.1093/intimm/dx1113>

Leslie, M. 2007. Mast cells show their might. *Science*. 317:614–616. <http://dx.doi.org/10.1126/science.317.5838.614>

Liu, F.T., J.W. Bohn, E.L. Ferry, H. Yamamoto, C.A. Molinaro, L.A. Sherman, N.R. Klinman, and D.H. Katz. 1980. Monoclonal dinitrophenyl-specific murine IgE antibody: preparation, isolation, and characterization. *J. Immunol.* 124:2728–2737.

Lozewicz, S., L. Greenwood, A.F. Walls, E. Gomez, and R.J. Davies. 1990. Mast cells in human bronchi are heterogeneous with respect to granule esterase activity. *Respir. Med.* 84:499–501. [http://dx.doi.org/10.1016/S0954-6111\(08\)80116-3](http://dx.doi.org/10.1016/S0954-6111(08)80116-3)

Martín-Cófreces, N.B., B. Alarcón, and F. Sánchez-Madrid. 2011. Tubulin and actin interplay at the T cell and antigen-presenting cell interface. *Front. Immunol.* 2:24. <http://dx.doi.org/10.3389/fimmu.2011.00024>

Mazzoni, A., R.P. Siraganian, C.A. Leifer, and D.M. Segal. 2006. Dendritic cell modulation by mast cells controls the Th1/Th2 balance in responding T cells. *J. Immunol.* 177:3577–3581. <http://dx.doi.org/10.4049/jimmunol.177.6.3577>

Mekori, Y.A., and A.Y. Hershko. 2012. T cell-mediated modulation of mast cell function: heterotypic adhesion-induced stimulatory or inhibitory effects. *Front. Immunol.* 3:6. <http://dx.doi.org/10.3389/fimmu.2012.00006>

Morelli, A.E., A.T. Larregina, W.J. Shufesky, M.L. Sullivan, D.B. Stolz, G.D. Papworth, A.F. Zahorchak, A.J. Logar, Z. Wang, S.C. Watkins, et al. 2004. Endocytosis, intracellular sorting, and processing of exosomes by dendritic cells. *Blood*. 104:3257–3266. <http://dx.doi.org/10.1182/blood-2004-03-0824>

Morva, A., S. Lemoine, A. Achour, J.O. Pers, P. Youinou, and C. Jamin. 2012. Maturation and function of human dendritic cells are regulated by B lymphocytes. *Blood*. 119:106–114. <http://dx.doi.org/10.1182/blood-2011-06-360768>

Otsuka, A., M. Kubo, T. Honda, G. Egawa, S. Nakajima, H. Tanizaki, B. Kim, S. Matsuoka, T. Watanabe, S. Nakae, et al. 2011. Requirement of interaction between mast cells and skin dendritic cells to establish contact hypersensitivity. *PLoS ONE*. 6:e25538. <http://dx.doi.org/10.1371/journal.pone.0025538>

Reuter, S., N. Dehzad, H. Martin, A. Heinz, T. Castor, S. Sudowe, A.B. Reske-Kunz, M. Stassen, R. Buhl, and C. Taube. 2010. Mast cells induce migration of dendritic cells in a murine model of acute allergic airway disease. *Int. Arch. Allergy Immunol.* 151:214–222. <http://dx.doi.org/10.1159/000242359>

Sadhu, C., H.J. Ting, B. Lipsky, K. Hensley, L.F. Garcia-Martinez, S.I. Simon, and D.E. Staunton. 2007. CD11c/CD18: novel ligands and a role in delayed-type hypersensitivity. *J. Leukoc. Biol.* 81:1395–1403. <http://dx.doi.org/10.1189/jlb.1106680>

Shelburne, C.P., H. Nakano, A.L. St John, C. Chan, J.B. McLachlan, M.D. Gunn, H.F. Staats, and S.N. Abraham. 2009. Mast cells augment adaptive immunity by orchestrating dendritic cell trafficking through infected

tissues. *Cell Host Microbe.* 6:331–342. <http://dx.doi.org/10.1016/j.chom.2009.09.004>

Shimaoka, M., and T.A. Springer. 2003. Therapeutic antagonists and conformational regulation of integrin function. *Nat. Rev. Drug Discov.* 2:703–716. <http://dx.doi.org/10.1038/nrd1174>

Shortman, K., and Y.J. Liu. 2002. Mouse and human dendritic cell subtypes. *Nat. Rev. Immunol.* 2:151–161. <http://dx.doi.org/10.1038/nri746>

Skokos, D., H.G. Botros, C. Demeure, J. Morin, R. Peronet, G. Birkenmeier, S. Boudaly, and S. Mécheri. 2003. Mast cell-derived exosomes induce phenotypic and functional maturation of dendritic cells and elicit specific immune responses *in vivo*. *J. Immunol.* 170:3037–3045. <http://dx.doi.org/10.4049/jimmunol.170.6.3037>

Smoligovets, A.A., A.W. Smith, H.J. Wu, R.S. Petit, and J.T. Groves. 2012. Characterization of dynamic actin associations with T-cell receptor microclusters in primary T cells. *J. Cell Sci.* 125:735–742. <http://dx.doi.org/10.1242/jcs.092825>

Soilleux, E.J., L.S. Morris, G. Leslie, J. Chehimi, Q. Luo, E. Levrony, J. Trowsdale, L.J. Montaner, R.W. Doms, D. Weissman, et al. 2002. Constitutive and induced expression of DC-SIGN on dendritic cell and macrophage subpopulations *in situ* and *in vitro*. *J. Leukoc. Biol.* 71:445–457.

Spendier, K., A. Carroll-Portillo, K.A. Lidke, B.S. Wilson, J.A. Timlin, and J.L. Thomas. 2010. Distribution and dynamics of rat basophilic leukemia immunoglobulin E receptors (Fc $\epsilon$ RI) on planar ligand-presenting surfaces. *Biophys. J.* 99:388–397. <http://dx.doi.org/10.1016/j.bpj.2010.04.029>

Springer, T.A., and M.L. Dustin. 2012. Integrin inside-out signaling and the immunological synapse. *Curr. Opin. Cell Biol.* 24:107–115. <http://dx.doi.org/10.1016/j.ceb.2011.10.004>

Suto, H., S. Nakae, M. Kakurai, J.D. Sedgwick, M. Tsai, and S.J. Galli. 2006. Mast cell-associated TNF promotes dendritic cell migration. *J. Immunol.* 176:4102–4112. <http://dx.doi.org/10.4049/jimmunol.176.7.4102>

te Riet, J., J. Helenius, N. Strohmeyer, A. Cambi, C.G. Figgdr, and D.J. Müller. 2014. Dynamic coupling of ALCAM to the actin cortex strengthens cell adhesion to CD6. *J. Cell Sci.* 127:1595–1606. <http://dx.doi.org/10.1242/jcs.141077>

Valentin-Torres, A., C.M. Ramirez Kitchen, H.S. Haller, and H.B. Bernstein. 2012. Bidirectional NK/DC interactions promote CD4 expression on NK cells, DC maturation, and HIV infection. *Virology.* 433:203–215. <http://dx.doi.org/10.1016/j.virol.2012.06.023>

van Gisbergen, K.P., C.A. Aarnoudse, G.A. Meijer, T.B. Geijtenbeek, and Y. van Kooyk. 2005a. Dendritic cells recognize tumor-specific glycosylation of carcinoembryonic antigen on colorectal cancer cells through dendritic cell-specific intercellular adhesion molecule-3-grabbing nonintegrin. *Cancer Res.* 65:5935–5944. <http://dx.doi.org/10.1158/0008-5472.CAN-04-4140>

van Gisbergen, K.P., I.S. Ludwig, T.B. Geijtenbeek, and Y. van Kooyk. 2005b. Interactions of DC-SIGN with Mac-1 and CEACAM1 regulate contact between dendritic cells and neutrophils. *FEBS Lett.* 579:6159–6168. <http://dx.doi.org/10.1016/j.febslet.2005.09.089>

van Gisbergen, K.P., M. Sanchez-Hernandez, T.B. Geijtenbeek, and Y. van Kooyk. 2005c. Neutrophils mediate immune modulation of dendritic cells through glycosylation-dependent interactions between Mac-1 and DC-SIGN. *J. Exp. Med.* 201:1281–1292. <http://dx.doi.org/10.1084/jem.20041276>

Walls, A.F., D.B. Jones, J.H. Williams, M.K. Church, and S.T. Holgate. 1990. Immunohistochemical identification of mast cells in formaldehyde-fixed tissue using monoclonal antibodies specific for tryptase. *J. Pathol.* 162:119–126. <http://dx.doi.org/10.1002/path.1711620204>

Wilson, B.S., S.L. Steinberg, K. Liederman, J.R. Pfeiffer, Z. Surviladze, J. Zhang, L.E. Samelson, L.H. Yang, P.G. Kotula, and J.M. Oliver. 2004. Markers for detergent-resistant lipid rafts occupy distinct and dynamic domains in native membranes. *Mol. Biol. Cell.* 15:2580–2592. <http://dx.doi.org/10.1091/mbc.E03-08-0574>

Xie, J., C.M. Tato, and M.M. Davis. 2013. How the immune system talks to itself: the varied role of synapses. *Immunol. Rev.* 251:65–79. <http://dx.doi.org/10.1111/imr.12017>

Yamashita, Y., N. Charles, Y. Furumoto, S. Odom, T. Yamashita, A.M. Gilfillan, S. Constant, M.A. Bower, J.J. Ryan, and J. Rivera. 2007. Cutting edge: genetic variation influences Fc $\epsilon$ RI-induced mast cell activation and allergic responses. *J. Immunol.* 179:740–743. <http://dx.doi.org/10.4049/jimmunol.179.2.740>

Yang, D., Q. Chen, O. Chertov, and J.J. Oppenheim. 2000. Human neutrophil defensins selectively chemoattract naive T and immature dendritic cells. *J. Leukoc. Biol.* 68:9–14.